《報文》 HWAHAK KONGHAK Vol. 18, No. 4, August 1980, pp. 215—226
(Journal of the Korean Institute of Chemical Engineers)

瞬間 蒸發現象에 관하여

——Flash 蒸發罐內에서 發生한 單一氣泡의 成長 및 運動에 관한 理論的 研究——

李 載 聖·李 成 圭

서울大學校 工科大學 化學工學科

(접수 1980. 2. 7)

A Study on Flashing Phenomena

——Growth and Rising of a Single Bubble in the Superheated Liquid of a Flash Stage——

Chai-sung Lee and Sunggyu Lee*

Department of Chemical Engineering
College of Engineering, Seoul National University, Seoul 151, Korea

(Received Feburary 7, 1980)

요 약

均一過熱液體內에서 發生한 單一氣泡에 對하여 運動量, 熱, 物質傳達의 諸關係와 氣泡壁에서의 非平衡效果를 考慮하여 氣泡成長 및 上昇機構를 Model 化하였으며, 非線型聯立微分方程式의 數值解를 求하였다. 그 結果로서, 氣泡成長後期뿐만 아니라, 中·初期에서도 適用시킬 수 있는 成長 및 上昇原理를 提示하였으며, 氣泡內部와 氣液境界面, 그리고 溫度境界層에서의 溫度, 壓力, 半徑의 動特性을 考察함으로써 單一氣泡의 履歷을 明白히 하였다. 또, 過熱度를 變化시켜서 얻은 結果를 比較檢討하였다.

Abstract

The behavior of a vapor bubble growing and rising simultaneously in a uniformly superh-

* Presently at the Department of Chemical Engineering, The University of Akron, Akron, Ohio

eated water was formulated taking into account of liquid inertia, heat conduction in the liquid and nonequilibrium effects at the vapor-liquid incerface. Neither experimental data nor overall solutions for the bubble behavior in flash stage have been available as yet. Some illustrative numerical solutions for the entire bubble history were obtained for various superheats. A comparison between our theory and other theoretical solutions was also presented and discussed.

I. Introduction

To clarify the physical mechanism of flash evaporation, various attempts have beed made.[1,2,3] Many current designs of MSF (Multi-Stage Flash) distillation plants arrange for the brine water to leave a pool in one stage via a specially designed rectangular orifice which leads into the base of riser in the succeeding stage. The brine water then flows up the top of the riser as a plume which descends in a pool. The schematic diagram of a single flash stage is shown in *Fig. 1*. Many investigations have shown that the temperature difference between the saturation temperature of vapor space plus the boiling point elevation and the outlet brine temperature is considerably large. The difference is called NETD (Nonequilibrium Temperature Difference) and the less is its value, the more is the profits attainable from the operation.

The effect of flashing differs in three processes of nucleation, growth, and rising of bubbles.

Basically, the phenomena of nucleation are believed to be the same for generation of bubbles in a flash stage and crystallization from a solution. In these instances, nucleation is a consequence of rapid local fluctuations on a molecular scale in a homogeneous phase that is in a state of metastable equilibrium. A study of nucleation phenomena using laser techniques is currently under way at the University of Glasgow, from which it is hoped nucleation rate function may be determined.[2]

The first solution for the problem of bubble growth was reported by Rayleigh. His solution neglected the heat transfer and considered only the dynamic effects. And it might be expected to be valid at the initial stage of growth. Later, Plesset and Zwick[4] and others[5] obtained the following asymptotic expression for the bubble radius as a function of time.

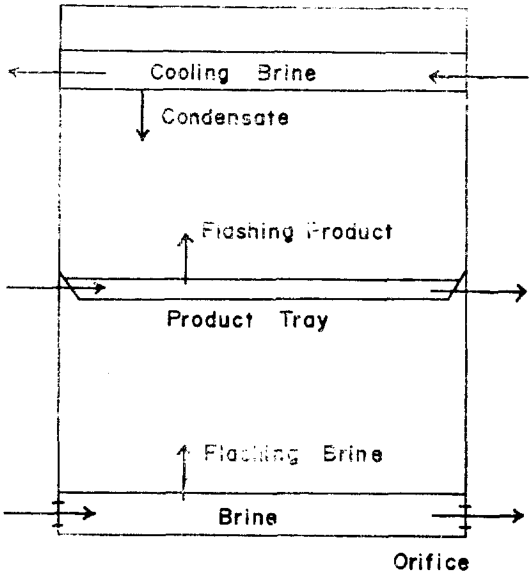

Fig. 1. Schematic diagram of a single flash stage

$$R_v = 2\, N_{Ja}(3\,\alpha t/\pi)^{\frac{1}{2}} \qquad (1)$$

where, N_{Ja} is the Jakob number

$$N_{Ja} = \frac{\rho_L C_{PL}(T_\infty - T_s)}{\rho_v \lambda} \qquad (2)$$

These solutions which assumed a purely heat transfer controlled process are valid for sufficiently large values of R_v. In their analyses, it is assumed that the temperature and chemical potential are equal in the vapor and liquid phases at the interface. The square root of time dependency of the bubble growth is in agreement with experimental measurements made by Dergarabedian and Kosky.[6,7] However, investigations have shown that bubbles are not in a thermodynamic equilibrium with the surrounding liquids, i.e. the vapor side temperature at the vapor-liquid interface is not the same as the liquid side temperature.[8,9]

For studying the flashing rate, the motion of vapor bubbles is a very important factor. The motion of constant size bubbles in liquids has been studied both theoretically and experimentally for a wide range of bubble radii. Pinto and Davis[11] analyzed the motion of simultaneously rising and growing bubbles in a superheated liquid, using Scriven's asymptotic solution of bubble radius.

The experimental difficulties of recording the bubble data during the initial stages of bubble growth prevented the precise determination of time scale.[10] Accordingly, almost no definitive experimental programs have been carried out.

The present theoretical study is directed to the clarification how the vapor is generated and released in the superheated liquid pool of the flash chamber. The purpose of this paper is to provide a complete systematic description of growing and rising processes for the combined effects of liquid inertia, heat transfer, and nonequilibrium. Some numerical solutions for the entire bubble history are illustrated for specific examples of bubbles in superheated water. Variations in temperatures and pressures with time are also presented.

Ⅱ. Analysis

A rigorous description of the bubble growth and the bubble's upward movement due to the buoyant force is not possible. It is our destiny to be contented with some sort of compromise so that an approximated model can be established. We may then proceed to write down the mathematical expressions to describe the behavior of the model.

It is necessary to make the following approximations or assumptions in order to frame up our model:

1. The shape of the bubble is spherical throughout the entire bubble life.[12]

2. The vapor side temperature at the vapor-liquid interface is lower than the liquid side temperature.

3. The vapor side temperature profile is a straight line normal to the interface (uniform vapor phase temperature).

4. There is a thermal boundary layer on the liquid side adjacent to the interface across which the main body temperature falls according to a second order profile, as shown in *Fig. 2*.

5. The external pressure exerting on the liquid pool remains constant.

6. The liquid is a Newtonian fluid and in a uniformly superheated state.

7. The vapor in the bubble follows the ideal gas law.

The definition of a model is completed when all necessary equations are written down as they follow.

1. Bubble Growth

In flash evaporation, bubbles are created by the expansion of entrapped gas of vapor at small cavities in the superheated liquid. These bubbles grow to a certain size, depending upon the surface tension at the liquid-vapor interface and the temperature and pressure.

Consider a spherical bubble growing in an infinte mass of uniformly superheated liquid. This model of a spherical bubble is justified by Saffman when its radius is less than 0.5 mm.[12] The balance of force at the bubble wall requires that

$$P_L(R_v)+2\sigma/R_v+\tau_{rr,L}(R_v)=P_v \quad (3)$$

where, $\tau_{rr,L}$ is the radial normal stress acting on the bubble interface due to the liquid viscosity and may be expressed by

$$\tau_{rr,L}(R_v)=4\mu_L\dot{R}_v/R_v \quad (4)$$

on the assumption that the liquid is a Newtonian fluid. But, the viscous term, $\tau_{rr,L}$ is very small compared with other terms and can be neglected. Therefore, the initial critical radius of bubble is defined as follow:

$$R_v(0)=R_{cr.}=\frac{2\sigma}{P_v(0)-P_\infty} \quad (5)$$

where, P_∞ and $P_v(0)$ are external pressure of a stage and initial pressure of bubble vapor, respectively. The dynamics start from the initial radius with a perturbation causing a departure from metastable equilibrium. As is widely known, the evolution of the vapor bubbles will depend upon the imposed pressure and temperature conditions.

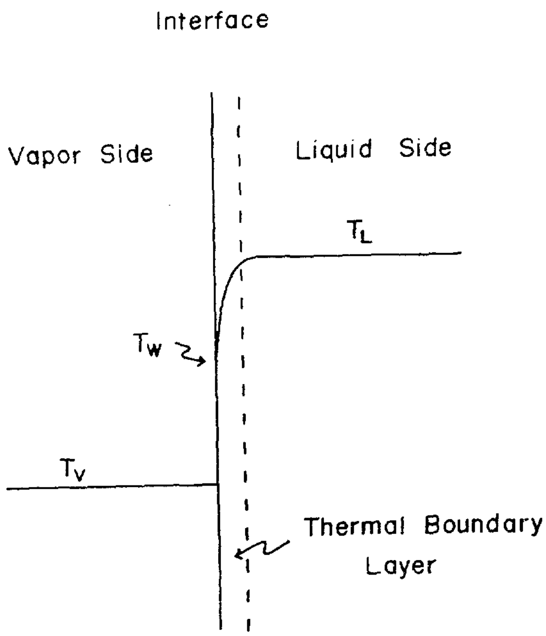

Fig. 2. Temperature profile for a bubble

(1) Work of nucleus formation

In general, the flashing process is critically dependent upon the presence of nuclei which permit the initial growth of the vapor bubbles. When a new phases B(vapor) is created from the mother phase A(liquid), the increase in Gibbs free energy per a nucleus may be derived as follows[13,14]:

$$\begin{aligned}\Delta G&=G-G_0\\&=(N_A\mu_A+N_B\mu_B+4\pi R_v^2\sigma)-(N_A+N_B)\mu_A\\&=4\pi R_v^2\sigma-(\mu_A-\mu_B)N_B\\&=4\pi R_v^2\sigma-\frac{(\mu_A-\mu_B)}{V_B}\cdot\frac{4}{3}\pi R_v^3\end{aligned} \quad (6)$$

where, V_B is the volume of one molecule in the vapor phase. Substituting $(\mu_A-\mu_B)/V_B=2\sigma/R_{cr.}$ yields,

$$\Delta G=4\pi\sigma\left((R_v^2-\frac{2}{3}\frac{R_v^3}{R_{cr.}}\right) \quad (7)$$

ΔG has a maximum value at $\left(\frac{\partial\Delta G}{\partial r}\right)=0$, corresponding to the desired value of $R_v=R_{cr.}$.

$$(\Delta G)_{max.}=\frac{1}{3}(4\pi R_{cr.}^2\sigma) \quad (8)$$

The result is plotted in *Fig. 3.* as a function of R_v. Since for all values of $R_v>R_{cr.}$, G decreases monotonously, further growth of the nucleus is spontaneous. That is to say, $R_{cr.}$ is the minimum-sized embryo which is

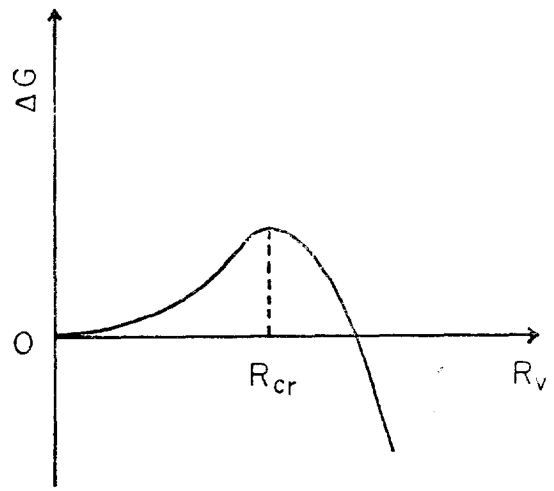

Fig. 3. Gibbs free energy vs. bubble radius

capable of initiating further spontaneous growth to produce the new phase.

(2) The net mass transfer equation

The simplified relationship for the net mass transfer rate is used:

$$W=k_g(P_w^*-P_v) \tag{9}$$

where, k_g is mass transfer coefficient

$$k_g=a\left(\frac{Mg_c}{2\pi RT_w}\right)^{\frac{1}{2}} \tag{10}$$

and P_w^* is saturation pressure corresponding to the wall temperature, T_w. The mass transfer coefficient, k_g, involves resistance factor, a, and it is the ratio of actual transfer rate to the value obtained from Knudsen,s kinetic theory.[15] Its value is initially close to unity and decreases with time. For an equilibrium to be attained, $P_v=P_w^*$, and this would require $a\to\infty$.

(3) Mass balance equation for the vapor

A mass balance over the growing vapor bubble yields

$$\frac{1}{4\pi R_v^2}\frac{d}{dt}\left(\frac{4}{3}\pi R_v^3\rho_v\right)=W \tag{11}$$

denoting the net mass flux at liquid-vapor interface by W. The vapor density can be rewritten in terms of the perfect gas law and is allowed to vary with time. Arranging Eq. (11) gives

$$\frac{3}{R_v}\frac{dR_v}{dt}+\frac{1}{P_v}\frac{dP_v}{dt}-\frac{1}{T_v}\frac{dT_v}{dt}=\frac{3\,WT_vR}{R_vP_vM} \tag{12}$$

(4) Continuity equation for the liquid

The equation of continuity for an incompressible liquid may be expressed in spherical coordinates as

$$\frac{1}{r^2}\frac{\partial}{\partial r}(r^2u_r)=0 \tag{13}$$

The integration of Eq. (13) gives the radial velosity u_r in terms of the bubble wall velosity $\dot{R}_v$:

$$u_r=\dot{R}_v(R_v/r)^2 \tag{14}$$

(5) Equation of motion for the liquid

In laminar flow regime, the equation of motion in the liquid with constant density may be expressed in spherical coordinates as[16]:

$$\rho_L\left(\frac{\partial u_r}{\partial t}+u_r\frac{\partial u_r}{\partial r}\right)=-\frac{\partial P}{\partial r}-|\nabla\cdot\tau|_r \tag{15}$$

The substitution of stress tensors into Eq. (15), followed by an integration with respect to r from R_v to reference radius r_0 (∞, in this case) at a particular time gives[17,18]

$$\ddot{R}_vR_v^2\left(\frac{1}{R_v}-\frac{1}{r_0}\right)+\dot{R}_v^2\left(\frac{R_v^4}{2r_0^4}-\frac{2R_v}{r_0}+\frac{3}{2}\right)=\frac{g_c}{\rho_L}\{P_L(R_v)-P_L(r_0)\} \tag{16}$$

The balance of forces at the liquid-vapor interferface is expressed by Eq. (3). Combining Eqs. (3) and (16) yields

$$\ddot{R}_v+\frac{3}{2}\frac{\dot{R}_v^2}{R_v}+4\mu_L\frac{\dot{R}_v}{\rho_LR_v^3}+\frac{2\sigma g_c}{\rho_LR_v^2}+\frac{(P_\infty-P_v)g_c}{\rho_LR_v}=0 \tag{17}$$

The instantaneous bubble size and its time derivative may be obtained by solving Eq. (17) with the initial conditions,

$$R_v(0)=R_{cr.}=\frac{2\sigma}{P_v(0)-P_\infty} \tag{18}$$

and $\dot{R}_v(0)=0$

which describes that initially the bubble with radius $R_{cr.}$ is in a force equilibrium at the boundary layer.

(6) Energy balance for the vapor

The internal energy content of the bubble accumulates through the heat and mass transfer from the surrounding liquid less the energy dissipation due to the expansion of bubbles.

$$\frac{d}{dt}\left(\frac{4}{3}\pi R_v^3\cdot\rho_v E_v\right) = 4\pi R_v n\cdot \Delta E - P_v\cdot 4\pi R_v^2 \dot{R}_v \qquad (19)$$

The net eaergy transfer rate per unit interface area, ΔE, is

$$\Delta E = a\sqrt{\frac{Mg_c}{2\pi RT_w}}\{P_w^* E_v(T_w,\ P_w^*) - P_v E_v(T_v,\ P_v)\}$$
$$= W\cdot E_v(T_v,\ P_v) + a\sqrt{\frac{Mg_c}{2\pi RT_w}}\cdot P_w^*\{E_v(T_w,\ P_w^*) - E_v(T_v,\ P_v)\} \qquad (20)$$

For an ideal gas,

$$E_v(T_w,\ P_w^*) - E_v(T_v,\ P_v) = C_v(T_w - T_v) \qquad (21)$$

$$\rho_v = MP_v/RT_v \qquad (22)$$

and Eq. (18) reduces to

$$\Delta E = W\cdot E_v(T_v,\ P_v) + a\sqrt{\frac{Mg_c}{2\pi RT_w}} P_w^* C_v(T_w - T_v) \qquad (23)$$

The substitution of Eqs. (22) and (23) into Eq. (19) gives:

$$\frac{MC_v}{RT_v}\frac{dT_v}{dt} = -\frac{3}{R}\frac{dR_v}{dt} + 3a\sqrt{\frac{Mg_c}{2\pi RT_w}}\cdot\frac{C_v}{R_v}\frac{P_w^*}{P_v}(T_w - T_v) \qquad (24)$$

(7) Energy balance for the liquid

The energy equation appropriate for the liquid phase is

$$\frac{\partial T_L}{\partial t} + \frac{R_v^2\dot{R}_v}{r^2}\frac{\partial T_L}{\partial r} = \frac{\alpha_L}{r^2}\frac{\partial}{\partial r}\left(r^2\frac{\partial T_L}{\partial r}\right) \qquad (25)$$

where we made use of Eq. (14) to express the convection velosity u_r in terms of $\dot{R}_v$. The initial and boundary condition for the energy equation are as follows:

$$T_L(r,\ 0) = T_\infty \qquad (a)$$
$$T_L(R_{TB},\ t) = T_\infty \qquad (b)$$
$$T_L(R_v,\ t) = T_w(t) \qquad (c) \qquad (26)$$
$$\left(\frac{\partial T_L}{\partial r}\right)_{r=R_{TB}} = 0 \qquad (d)$$
$$\left(\frac{\partial T_L}{\partial r}\right)_{r=R_v} = \frac{\lambda}{k}W \qquad (e)$$

Eq. (26-a) shows that the liquid is initially at a uniform temperature T_∞. Eq. (26-b) indicates that the liquid temperature at a distance beyond the thermal boundary layer thickness from the bubble surface remains unchanged at T_∞. Eq. (26-c) indicates that the temperature of water in contact with the bubble is the same as the bubble wall temperature. And Eq. (26-e) is obtained from the conservation of energy at the bubble wall by neglecting the gas velosity relative to $\dot{R}_v$ and temperature gradient in gas phase. But, it appeared that a complete analytic solution was not possible and that the use of a temperature distribution of liquid would be more profitable.

Assuming a second-order temperature distribution, which was proposed by Bornhorst and Hatsopoulos[9], we obtain

$$T_L - T_w = (T_\infty - T_w)\cdot\left\{\frac{2(r-R_v)}{\delta} - \left(\frac{r-R_v}{\delta}\right)^2\right\} \qquad (27)$$

where, $\delta = R_{TB} - R_v$ (28)

This temperature distribution satisfies all the boundary conditions except (e), so further arrangements are inevitable.

Combining Eqs. (25) and (27) and then integrating from R_v to R_{TB}, we obtain

$$-\frac{1}{(T_\infty - T_w)}\frac{dT_w}{dt}\left\{\frac{1}{3} + \frac{1}{6}\left(\frac{R_{TB}-R_v}{R_v}\right) + \frac{1}{30}\left(\frac{R_{TB}-R_v}{R_v}\right)^2\right\} + \frac{1}{(R_{TB}-R_v)}\left(\frac{dR_{TB}}{dt} - \frac{dR_v}{dt}\right)\left\{\frac{1}{3} + \frac{1}{3}\left(\frac{R_{TB}-R_v}{R_v}\right) + \frac{1}{10}\left(\frac{R_{TB}-R_v}{R_v}\right)^2\right\}$$

$$+\frac{1}{R_v}\frac{dR_v}{dt}\left\{\frac{2}{3}-\frac{1}{6}\left(\frac{R_{TB}-R_v}{R_v}\right)\right\}=\frac{2\alpha_L}{(R_{TB}-R_v)^2} \quad (29)$$

Boundary condition (26-e) may be expressed as

$$\left(\frac{\partial T_L}{\partial r}\right)_{r=R_{TB}}=\frac{2(T_\infty-T_w)}{(R_{TB}-R_v)} \quad (30)$$

Differentiating Eq. (30) with respect to time forms the additional relationship.

$$\frac{1}{R_{TB}-R_v}\frac{dT_w}{dt}+\frac{T_w-T_\infty}{(R_{TB}-R_v)^2}\left(\frac{dR_v}{dt}-\frac{dR_{TB}}{dt}\right)+\frac{\lambda}{2\kappa}\frac{dW}{dt}=0 \quad (31)$$

2. Rising of a Bubble

Consider a vapor bubble simultaneously growing and moving through a uniformly superheated liquid. The equation of motion for the vapor bubble is given by the Basset equation,

$$\frac{d}{dt}\left\{\left(\rho_v\frac{4}{3}\pi R_v^3 v_r\right)+\left(\frac{1}{2}\rho_L\frac{4}{3}\pi R_v^3 v_r\right)\right\}=(\rho_L-\rho_v)\frac{4}{3}\pi R_v^3 g-C_D\pi R_v^2\frac{\rho_L v_r^2}{2} \quad (32)$$

The added mass term, $\frac{1}{2}\rho_L\frac{4}{3}\pi R_v^3 v_r$, which was first introduced by Basset, represents the momentum of liquid accelerated with the bubble. Applying the ideal gas law to the vapor density, Eq. (32) becomes

$$\left(\frac{MP_v}{RT_v}+\frac{1}{2}\rho_L\right)\frac{dv_r}{dt}+\frac{3v_r}{R_v}\left(\frac{MP_v}{RT_v}+\frac{\rho_L}{2}\right)\frac{dR_v}{dt}+\frac{Mv_r}{RT_v}\frac{dP_v}{dt}-\frac{MP_v v_r}{RT_v^2}\frac{dT_v}{dt}=\left(\rho_L-\frac{MP_v}{RT_v}\right)g-C_D\frac{3}{8}\frac{\rho_L v_r^2}{R_v} \quad (33)$$

We shall assume that at any point in time the drag coefficient of the bubble is that of a bubble of constant size moving at its terminal velocity. This assumption was justified by Davis and Pinto.[11] Then, the drag coefficients are obtained from terminal velocity correlations for constant size bubbles. For the smaller bubbles whose radii are less than 0.4 mm, the drag coefficient is obtained from Levich's terminal velocity expression[11,19],

$$C_D=\frac{216\nu^2}{gR_v^3} \qquad (R_v\leq 0.4\text{ mm}) \quad (34)$$

For the larger bubbles whose radii are larger than 0.7 mm, the Peebles and Garber terminal velocity expression is used[19]:

$$C_D=\frac{8}{3}\frac{R_v^2}{1.82}\frac{\rho_L g}{\sigma g_c} \qquad (R_v\geq 0.7\text{ mm}) \quad (35)$$

Combining Eqs. (33), (34), and (35) gives the equation of motion for the bubble. Appropriate initial conditions are as follows:

$$\text{at } t=0, \quad v_r=0, \quad \frac{dv_r}{dt}=0 \quad (36)$$

Ⅲ. Numerical Solution

1. Nonequilibrium Solution

In previous sections, we have six time-dependent unknowns, T_v, T_w, P_v, R_v, R_{TB}, and v_r. Six nonlinear ordinary differential equations, (12), (17), (24), (29), (31), and (33) constitute a complete system of a simultaneously growing and rising bubble in terms of six time-dependent variables. Once their initial perturbed values are given, the complete history of bubble is obtained uniquely. Actually, a very small step increase in the imposed external pressure, $\Delta P_\infty/P_\infty=10^{-5}$, was used to initiate the bubble growth.

A modified Runge-Kutta 4th order integration scheme was used to solve the system simultaneously. The imposed initial conditions and time increments must be carefully determined, for the round-off errors might cause reversing the driving force in the early stage of bubble growth. A time step size of 10^{-8} sec was found to be satisfactory for good accuracy and stability of the solutions.

2. Equilibrium Solution

In most previous works[4,5,6,7], it has always been assumed that the pressure and temperature at the interface are related by saturation conditions. In other words, vapor in the bubble was assumed to be always saturated at liquid interface temperature. Accordingly, this assumption causes large deviations from the actual growth behavior, especially at low pressure.

In order to compare with our nonequilibrium solution, numerical integrations for this equilibrium assumption were also performed. A time step size of 10^{-6} sec was used and the accuracy of the solution was checked by using different step sizes.

Ⅳ. Results and Discussion

Numerical solutions about the time-dependent behavior of bubbles in the superheated water are presented by a parametric study for the system of various superheats.

A comparison between our present theory and other theoretical solutions is presented in *Fig. 4*. The bubble growth characteristic curve may be described as follows by considering the three regions indicated in the figure.

Region 1 (Accelerating Region)-At the initial stage of growth, the inertial effect is predominant, and the Rayleigh solution agrees well with our solution.

Region 2 (Nonequilibrium Region)-Bubbles are growing at almost constant rate and the nonequilibrium effect is very important in this region. The nonequilibrium effect is the difference between the equilibrium curve and the curve corresponding to the nonequilibrium solution. The length of constant rate period

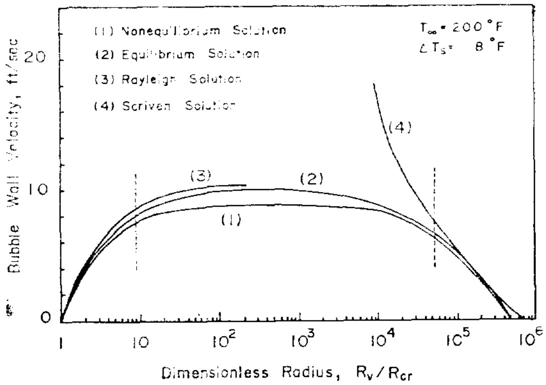

Fig. 4. Comparison of present theory with other theoretical solutions

is decreasing with increasing superheats.

Region 3 (Falling Rate Region)-If a bubble grows to a certain size, its growth rate begins to decrease. The purely heat transfer controlling Scriven's solution becomes to closely coincide with our curve at a later stage, with some necessary translation along the time scale.

Fig. 5. shows plots of the bubble wall velosity versus the dimensionless bubble radius. The dimensionless radius is the ratio of the instantaneous bubble radius to the initial critical radius. Each curve is for a fixed value of T_∞(200°F) while superheat temperature, ΔT_s, is varied from 8°F to 60°F, corresponding to the external pressure. As expected, the bubble wall velosity increases with an increase in ΔT_s or a decrease in P_∞.

Time variations in pressure and temperaure of a vapor bubble are presented in *Figs. 6, 7* and *8*. Pressure of bubble is also plotted against the dimensionless radius in *Fig. 9*.

Fig. 10 presents plots of the thermal boundary layer thickness versus time in log-log scale. It should be noted that the thermal boundary layer thickness is proportional to the square-root of time and very small compared with the corresponding bubble radius.

Fig. 11 shows the ascending velosity predictions for bubbles simultaneously growing and rising in the superheated water. It can be seen from the figure that bubbles are almost motionless at the nucleation sites until they grow to a certain size. For low superheats, there is more rapid acceleration initially than for high superheats. For higher superheats, the growth rate is so large that the maximum velosity is quickly reached. These results are consistent with Darby's observations at early times and with Pinto's large-time solution at later times.

In order to check our present theory, bubble-growth and rising measurements are

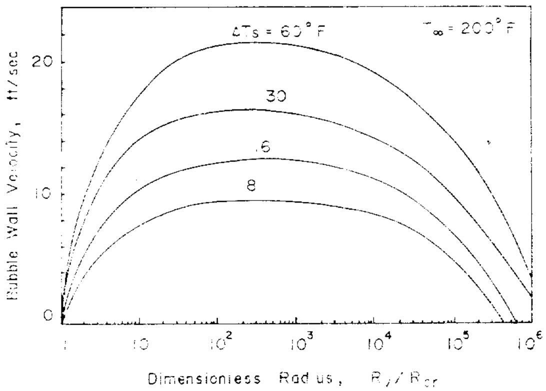

Fig. 5. The bubble growth behavior for various superheats

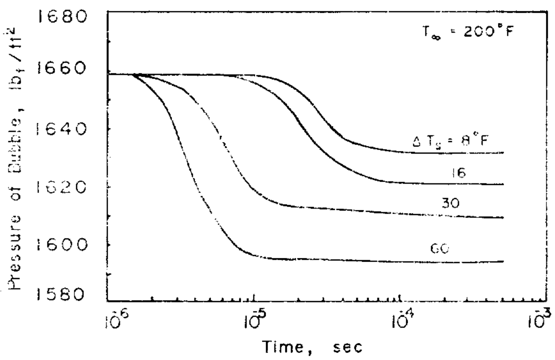

Fig. 6. Time variations of the pressure of a bubble

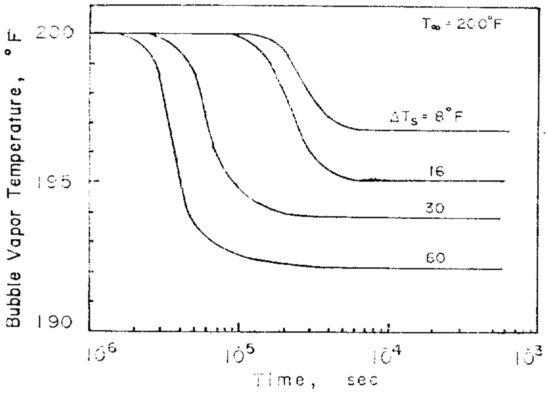

Fig. 7. Time variations of the temperature of a bubble

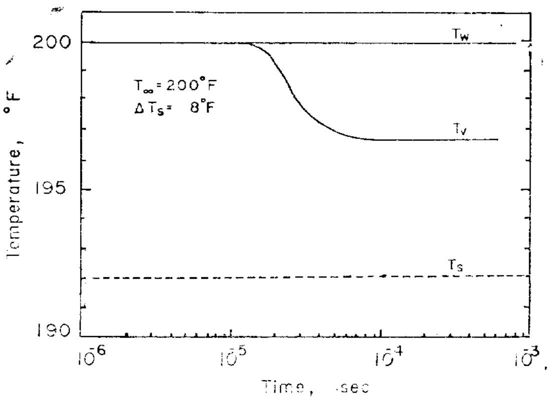

Fig. 8. Time variations of T_v and T_w

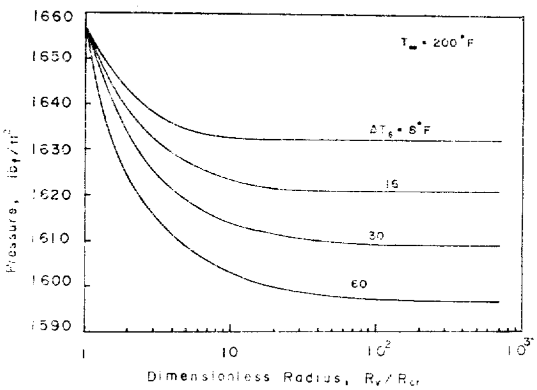

Fig. 9. Pressure vs. dimensionless radius

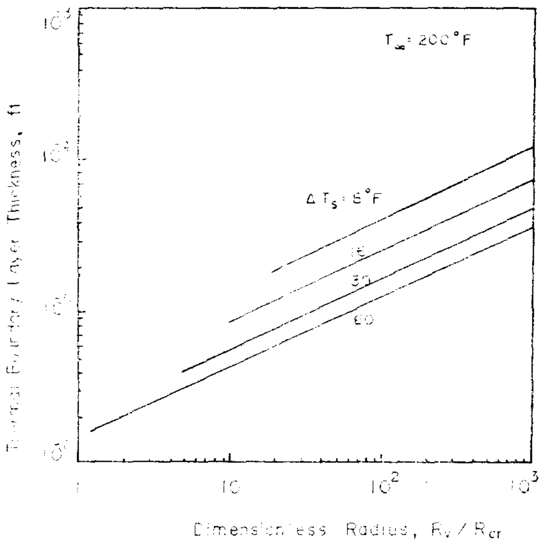

Fig. 10. Thermal boundary layer thickness vs. dimensionless radius

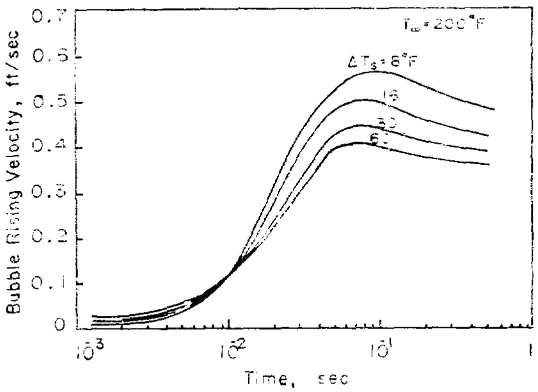

Fig. 11. Bubble rising velocity predictions

required at flash stages. For this purpose, techniques of synchronization of reducing pressure and recording time are to be developed.

Ⅴ. Conclusion

In our study of the flashing phenomena of saline water we have substituted it with superheated liquid water and focused our attention on a bubble embryo which has attained a certain minimum critical rtdius beyond which the bubble is considered to grow spontaneously.

One of the two previous theories on bubble growth took only the dynamic effect into consideration without taking heat transfer effect into account, while the other assumed a pourely heat transfer controlled process in calculating the bubble growth rate.

In this work, a more complete description of the bubble growth was attempted by adding mass transfer rate equation between the vapor and the bubble wall, mass balance and the energy balance equations for the vapor phase in extra to the previously raised equations in modeling the flash stage as summarized in *Table 1*. The scope of this work was further extended to calculating the rising velocity of a bubble growing under the conditions just have been described.

Because the system is under unstable superheated liquid state a small perturbation such as slightly changing the external pressure will suffice to initiate the bubble growth.

This work consists essentially of solving numerically the six simultaneous nonlinear ordinary differential equations with a time step of 10^{-8} seconds that gave a set of good stable solution. The solution depicts the complete time behavior of temperatures of vapor bubble and vapor-liquid interface, the radius of the bubble and the peripheral radius of the thermal diffusion layer together with the rising velocity of the bubble.

The computer used was FACOM 230-28 S and one set of computation took 3 hours and 8 minutes of CPU time.

It should, however, be mentioned that

Table 1. Three Different Models for Bubble Growth Behavior

Name of Equations	Rayleigh	Scriven	Our work
1. Mass Transfer Eq.			×
2. Mass Balance Eq. for the Vapor			×
3. Continuity Eq. for the Liqud	×	×	×
4. Eq. of Motion for the Liqiuid	×		×
5. Engrgy Balance for the Vapor			×
6. Energy Balance for the Liquid		×	×

although there is definitely an effect of bubble growth on the rising velocity, the reverse, that is the effect of rising velocity on the bubble growth could not be correlated. The concept reciprocal to hindered settling in the case of violent bubble evolutions is beyond the scope of this work. The problem of neucleation, that is the formation of bubble embryos smaller than the critical radius R_{cr} is still to be worked out. The shape which a large bubble will actually assume while rising through the liquid can not be a true sphere. It may be far different from a sphere and thus the entire analysis based on a spherical bubble assumption may grossly be in error unless a certain shape factor is introduced.

Furthermore the results were not checked by experimental measurments because of the difficulty in doing so.

It may however be said that the results of the theoretical analyses performed here gave a very important behavior of bubble growth, particularly when one note on the accelerating region, constant rate region and falling rate region in the history of bubble growth.

It must noted also that as the superheat increases, or the external pressure decreases, that is, as the degree of nonequilibrium deepens, the rate of bubble growth increases rapidly reaching a height and then declines as the bubble size gets large.

Both temperature and pressure of the bubble attains their final values determined by the degree of nonequilibrium as a matter of an instant, namely in approximately several hundred thousandth of a second after the growth is initiated. The bubble pressure reaches its final value when its size grows one hundred times the critical size.

The liquid side thermal boundary layer thickness gets increasingly thinner as the superheat increases, but it gets thicker as the bubble size increases.

Finally the bubble rising velosity reaches its maximum value in about one tenth of a second, but the bubble stays almost motionless at around one hundredth of a second and earlier.

One could easily realize how difficult it would be to actually prove these predictions by experiments. But we hope to be able to accomplish this one day.

Notation

a mass transfer resistance factor
C_D drag coefficient, dimensioless
C_{pL} heat capacity of liquid at constant pressure, Btu/lb·°F
C_v heat capacity of vapor at constant volume, Btu/lb·°F
E internal energy per mass, Btu/lb
G Gibbs free energy, Btu/lb
g gravitational acceleration, ft/sec²
g_c gravitational conversion factor

k thermal conductivity of liquid, Btu/ft-sec-°F
k_g mass transfer coefficient, lb/lb_f-sec
M molecular weight of vapor
N_A, N_B number of molecules of phase A and B, respectively
N_{Ja} Jakob number, dimensionless
P pressure, lb_f/ft^2
P_v pressure in vapor
P_w* saturation pressure at $T=T_w$
$P_v(0)$ initial pressure of vapor bubble
P_∞ pressure at infinity
R gas constant
$R_{cr.}$ initial critical radius, ft
R_{TB} thermal boundary layer radius, ft
R_v instantaneous bubble radius, ft
$R_v(0)$ initial critical radius, ft
$\dot{R}_v$ time derivative of bubble radius, ft/sec
r radial distance
r_0 reference radius
T temperature, °F
T_L temperature of liquid
T_s liquid saturation temperature at $P=P_\infty$
ΔT_s superheat temperature
T_v temperature of vapor bubble
T_w bubble wall temperature
T_∞ temperature of liquid at infinity
t time
u_r radial velosity of liquid, ft/sec
v_r bubble rising velosity, ft/sec
W net mass flux at liquid-vapor interface, lb/sec-ft²

Greek letters

α_L thermal diffusivity of liquid, ft²/sec
δ thermal boundary layer thickness, ft
λ heat of vaporization, Btu/lb
μ_L liquid viscosity, lb/ft-sec
μ_A, μ_B chemical potential of A, B
ν kinematic viscosity of liquid, ft²/sec
σ surface tension of liquid, lb_f/ft
ρ density, lb/ft³
$\tau_{rr'L}$ radial normal stress acting on the bubble interface

References

1. Electronic Associates, Inc., "Simulation of a multi-stage flash module," Report to the U.S. Department of Interior (1971).
2. A.N. Dickson and A.J. Addlesee, 3rd International Symposium on fresh Water from the Sea, 4(1970), 31.
3. O. Miyatake and et. al., 日本海水學會誌. 26, No. 4(1872), 189.
4. M.S. Plesset and S.A. Zwick, J. Appl. Phys., **25**(1954), 493.
5. L.E. Scriven, Chem. Eng. Sci., **10**(1959), 1.
6. P. Dergarabedian, J. of Fluid Mechanics, **9**(1960), 39.
7. P.G. Kosky, Chem. Eng. Sci., **23**(1968), 695.
8. W.J. Bornhorst and G.N. Hatsopoulos, A.S.M.E., **34**(1967), Ser. E No. 4, 840.
9. W.J. Bornhorst and G.N. Hatsopoulos, A.S.M.E., **34**(1967), Ser. E No. 4, 847.
10. T. Theofanous, L. Bias and H.S. Isbin, Chem. Eng. Sci., **24**(1969), 885.
11. Y. Pinto and E.J. Davis, AIChE J., **17** (1971), 1452.
12. 日本機械學會編, "沸騰熱傳達," 第2, 3章 (1965).
13. K. Victor and La Mer, I. and E.C., **44** (1952), 1270
14. L. Bernath, I and E.C., **44**(1952), 1310.
15. R.B. Holden and R. Speiser, J. Am. Chem. Soc. **70**(1948), 3897.
16. R.B. Bird, W.E. Stewart and E.N. Lightfoot, "*Transport Phenomena,*" Chap. 3, Wiley, N.Y. (1960).
17. L.S. Tong, "*Boiling heat transfer and Two-phase flow,*" Chap. 2, Wiley, N.Y. (1967).
18. W.J. Yang and H.C. Yeh, AIChE J., **12** (1966), 927.
19. F.N. Peebles and H.J. Garber, Chem. Eng.-Progr. **49**(1952), No. 2, 88.